ISSN 1330-3651
UDC/UDK 53.088.3:519.245

VALIDATION OF THE REALISED MEASUREMENT UNCERTAINTY IN PROCESS OF PRECISE LINE SCALES CALIBRATION

Srđan Medić, Živko Kondić, Biserka Runje

Original scientific paper

The Laboratory for Precise Measurement of Length, which is at the same time the Croatian National Laboratory for Length (in text Laboratory) takes part in CIPM MRA (Comité International des Poids et Mesures, Mutual Recognition Arrangement) comparisons of length standards, which include line scales as very important standards of length. When the results reported in the comparisons, it is necessary to state the estimated measurement uncertainty. Recently, the Monte Carlo simulations (MCS) have been increasingly applied in the field of estimation measurement uncertainties. The paper presents validation of the realised measurement uncertainty by GUM method in process of precise line scales calibration using the MCS method. The MCS method is based on random number generation from the probability density functions for each input value and forming of experimental probability density function of the output value. Also, the paper presents obtained results of the international comparison measurement which representing a real validation of the device and evaluated measurement uncertainty.

Keywords: *calibration, line scales, measurement uncertainty, Monte Carlo simulation*

Validacija realizirane mjerne nesigurnosti u postupku umjeravanja preciznih mjernih skala

Izvorni znanstveni članak

Laboratorij za precizna mjerenja dužina koji je ujedno i Nacionalni laboratorij za duljinu sudjeluje (Laboratorij) CIPM MRA (Comité International des Poids et Mesures, Mutual Recognition Arrangement) ključnim usporedbama etalona duljine među kojima su od posebnog značaja i precizne mjerne skale. U usporedbenim mjerenjima pri iskazivanju rezultata mjerenja, neophodno je dati i procjenu mjerne nesigurnosti. U novije vrijeme, Monte Carlo simulacije (MCS) imaju sve veću primjenu u procjeni mjernih nesigurnosti. U radu se prezentira validacija realizirane mjerne nesigurnosti GUM metodom upotrebom MCS metode. MCS metoda temelji se na generiranju slučajnih brojeva iz funkcija gustoće vjerojatnosti za svaku ulaznu veličinu i stvaranju eksperimentalne funkcije gustoće vjerojatnosti izlazne veličine kombinirajući različite razdiobe kojima su definirane ulazne veličine. Isto tako, u radu se prezentiraju rezultati međunarodnog usporedbenog mjerenja koji predstavljaju stvarnu validaciju mjernog uređaja i procijenjene mjerne nesigurnosti.

Ključne riječi: *mjerna nesigurnost, mjerne skale, Monte Carlo simulacija, umjeravanje*

1 Introduction

Monte Carlo simulations are a class of computational algorithms that rely on repeated random sampling to compute their results. The Monte Carlo method was coined in the 1940s by John von Neumann, Stanislaw Ulam and Nicholas Metropolis, while they were working on nuclear weapon projects (Manhattan Project) in the Los Alamos National Laboratory. It was named in homage to the Monte Carlo Casino, a famous casino where Ulam's uncle would often gamble away his money [1÷9]. Monte Carlo simulations are often used in computer simulations of physical and mathematical systems. These methods are most suited to calculation by a computer and tend to be used when it is infeasible to compute an exact result with a deterministic algorithm. Monte Carlo simulations are especially useful for simulating systems with many coupled degrees of freedom, such as fluids, disordered materials, strongly coupled solids, and cellular structures. In recent time, Monte Carlo simulations (MCS) have been increasingly used in the evaluation of measurement uncertainty so it is issued addition of a GUM: GUM 101:2008 Propagation of distributions using a Monte Carlo simulation [2].

Compared to the standardized procedures (GUM method) of calculating the measurement uncertainty, this method has a whole range of advantages, but it also has some disadvantages. However, according to the experience acquired at the Laboratory for Precise Measurement of Length (LFSB) the advantages of this method are greater, and especially at levels where it is necessary to calculate the measurement uncertainty and the knowledge (statistics, differential calculus) and experience are lacking. In other obtained result is experienced visually and the uncertainty calculus often turns into "fun". It is precisely the impossibility of visual presentation of the measurement uncertainty which is probably the worst drawback of the GUM method.

Further, an example of comparison application of the MSC method with GUM method is presented, in the calibration procedure of precise line scale length of 100 mm, participating in the EURAMET Key Comparison, EURAMET.L-K7 "Calibration of line scales" (a project shared by the leading calibration institutes in the world).

2 Estimation of measurement uncertainty by MCS method

MCS method is based on generating random numbers from the probability density function for each input variable x_i and the creation of experimental probability density function of output values Y by combined different distributions which are defined input variables. The procedure is repeated M times, and on this way is created experimental probability density function of output values which is based on $M \times Y$ values. From experimental probability density function are estimated output values y, the estimated standard deviation, and interval estimation

$$\left(Y_{(\frac{1-P}{2},M)}, Y_{(\frac{1+P}{2},M)} \right).$$

MCS can be stated as a step-by-step procedure [9]:

1. Select the number M of Monte Carlo trials to be made;
2. Generate M vectors, by sampling from the assigned PDFs, as realizations of the (set of N) input quantities x_i;

3. For each such vector, form the corresponding model value of Y, yielding M model values;
4. Sort these M model values into strictly order using the sorted model values to provide G;
5. Use G to form an estimate y of Y and the standard uncertainty $u(y)$ associated with y;
6. Use G to form an appropriate coverage interval for Y, for a stipulated coverage probability p.

2.1 Conditions for the valid application of the described Monte Carlo method

The propagation of distributions implemented using MCS can validly be applied, and the required summary information subsequently determined, under the following conditions:

a) f is continuous with respect to the elements X_i of vector $\boldsymbol{X}$ in the neighborhood of the best estimates x_i of the X_i
b) the distribution function for Y is continuous and strictly increasing
c) the Probability density function of output value Y is:
- continuous over the interval for which this PDF is strictly positive,
- unimodal (single-peaked) and
- strictly increasing (or zero) to the left of the mode and strictly decreasing (or zero) to the right of the mode
d) if expectation $E(Y)$ and variance $V(Y)$ exist;
e) if is used a sufficiently large value of M.

3 Measurement device for calibrating of line scales

Calibration of the line scales at the level of measurement uncertainties of the order of value U = 0,1 μm, k = 2 represents today still a world problem, although these levels of measurement uncertainties are necessary in the context of ensuring the traceability. In the previous methods of calibrating the line scales that were used at Laboratory for precise measurements of length, it was impossible to avoid the influence of the measurer in the calibration procedure of the line scale. Therefore, during 2003 the Laboratory started to design their own optoelectronic system for the calibration of line scales [6].

The measuring range of the device is 800 mm and it is primarily intended for the calibration of line scales. The sighting process is done by means of a microscope with a digital CCD camera Olympus DP 70 with 12,5 Megapixels. The microscope is fitted with lens of different magnification (10×, 20×, 50×). The lenses are selected in compliance with the object of measurement.

The measuring system used is the laser interferometer (Renishaw ML 10). The basis of the Renishaw Laser Interferometer system is He-Ne Laser operating at a wavelength of 0,663 μm. Measurement device for calibrating of line scales is presented in Fig. 1. In order to achieve order in the above-mentioned measurement uncertainties, it is necessary to use software in the process of detecting the line centre of the measuring scale reference to requirement limits. The software solution functions in such a way that all the pixels of a certain image are transmitted into a black & white combination and then the position of the line centre is calculated by arithmetic algorithms.

The software solution provides the exact position of the line centre in pixels. In order to convert the values in pixels into the length values, it is necessary to calibrate the pixel size.

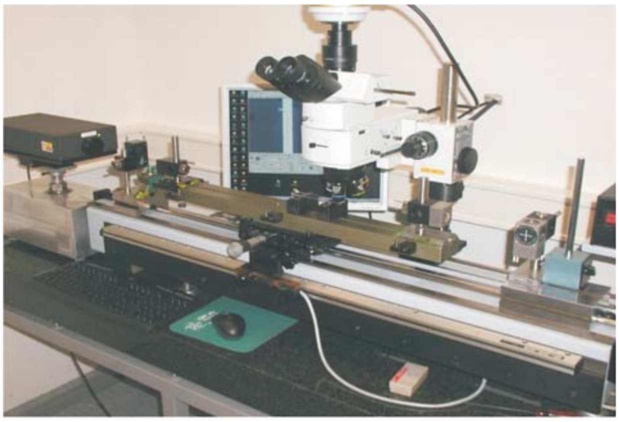

Figure 1 System for calibration of precise line scales

4 Calculation of the measurement uncertainty by applying GUM and MCS method

The precise line scales are calibrated in the range of nanometrology and as such are subject to various sources of uncertainties that need to be reduced to a minimum.

As a part of research on the impact of measurement uncertainty the following was investigated: the position of laser light sources and optical components, minimizing Abbe's error, the determination of the middle line of line scales, alignment of line scale and laser beam, straightness movement of table, pitch, roll and yaw angles, environmental conditions affect the laser wavelength and the geometry of device and the impact of losing focus while moving of table. The mathematical model of measurement has been given by expression (1) [8]:

$$\begin{aligned} L_{\mathrm{MS}} &= (N_2 - N_1)\frac{\lambda}{2n_{\mathrm{air}}} - (\delta l_{\mathrm{n2}} - \delta l_{\mathrm{n1}}) + \delta l_{\mathrm{DP}} + \delta l_{\mathrm{li}} + \\ &+ \delta l_{\mathrm{A}z} + \delta l_{\mathrm{A}y} + L \cdot \alpha_{\mathrm{s}} \cdot \Delta t_{\mathrm{s}} + \delta l_{\mathrm{sh}} + \delta l_{\mathrm{sv}} + \delta l_{\mathrm{ai}} + \\ &+ \delta E_{\mathrm{alg}} + \delta e_{\mathrm{fok}} + \delta l_{\mathrm{opt}} + \delta l_{\mathrm{s}E}. \end{aligned} \tag{1}$$

Where:

N_i - Number of wavelengths
λ - Laser wavelength
n_{air} - Refractive index of air
δl_{ni} - Interferometer nonlinearity
δl_{DP} - Dead path influence
δl_{li} - Interferometer cosine error
$\delta l_{\mathrm{A}z}$ - Abbe offset in z and pitch
$\delta l_{\mathrm{A}y}$ - Abbe offset in y and yaw
L - Nominal length of line scale
α_{s} - Thermal exp. Coefficient
Δt_{s} - Deviation scale temperature from 20 °C
δl_{sh} - Scale alignment horizontally
δl_{sv} - Scale alignment vertically
δl_{ai} - Scale support influence
δE_{alg} - Line quality influence
δe_{fok} - Focus loosing influence
δl_{opt} - Uncertainty of measure. optics due to temp. dev.
$\delta l_{\mathrm{s}E}$ - Reproducibility of line detection.

The yields of components of the standard uncertainty for the line scale of 100 mm are presented in Tab. 1.

Table 1 Yields of components of standard uncertainty

Source and component of uncertainty x_i	Distr.	Amount of stand. uncertainty $u(x_i)$	$c_i = \frac{\partial \delta L}{\partial x_i}$	Yield to measure. uncertainty /nm L in mm
Abbe offset in z and pitch, δl_{Az}	R	16,8 nm	1	16,8
Abbe offset in y and yaw, δl_{Ay}	R	4,3 nm	1	4,3
Laser wavelength, $\delta\lambda$	R	0,03	L	$0{,}03 \cdot L$
Air temperature, t_{air} / °C	R	0,12 °C	$9{,}5\times10^{-7} \cdot L$	$0{,}112 \cdot L$
Air pressure, p_{air}	R	13 Pa	$2{,}7\times10^{-7} \cdot L$	$0{,}035 \cdot L$
Relative humidity, RH_{air}	R	0,06	$8{,}5\times10^{-7} \cdot L$	$0{,}050 \cdot L$
Edlen equation uncertainty, δn_{air}	N	2×10^{-8}	L	$0{,}020 \cdot L$
Deadpath, δl_{DP}	R	1,8 nm	1	1,8
Interferometer nonlinearity, δl_{ni}	U	3 nm	1	3
Interferometer cosine error, δl_{li}	R	$0{,}48 \cdot L$	1	$0{,}48 \cdot L$
Deviation scale temperature from 20 °C, Δt_s /K	N	0,12 °C	$5\times10^{-7} L$	$0{,}06 \cdot L$
Thermal exp. Coef., α_s, 1/K	R	$0{,}289\times10^{-7}$	$L \cdot 0{,}5$	$0{,}0145 \cdot L$
Scale alignment horiz., δl_{sh}	R	$0{,}001 \cdot L$	1	$0{,}001 \cdot L$
Scale alignment vert, δl_{sv}	R	$0{,}0023 \cdot L$	1	$0{,}0023 \cdot L$
Scale support, δl_{ai}	R	$0{,}0058 \cdot L$	1	$0{,}0058 \cdot L$
Line quality, δE_{alg}	N	6,4 nm	1	6,4
Focus loosing, δe_{fok}	N	18 nm	1	18
Measurement optics, δl_{opt}	R	58 nm	1	58
Interferometer resolution, N	R	0,003	$\lambda/2$	1
Reproducibility of line detection, δl_{sE}	N	11,6 nm	1	11,6
Combined variance			$u^2 = (65^2 + 0{,}5^2 \cdot L^2)$ nm, L in mm	
Linearised expanded measurement uncertainty U, P = 95 %, k = 2			$U = (130 + 0{,}66 \cdot L)$ nm, L in mm	

Calculation of the measurement uncertainty (validation) has also been performed, by means of MCS method. Probability density function of the output value has been obtained by M = 100000 simulations. The probability density function $g(x_i)$ has been simulated by the MCS method based on the expression (1) where are [8]:

$$n_{air} = 1 - 3{,}634\times10^{-10} \cdot h \cdot e^{AT^2 + BT + C + DT^{-1}} + \delta_e + \frac{2{,}878\times10^{-9} \cdot p \cdot \left[1 + 10^{-8}(0{,}601 - 0{,}00972 \cdot t) \cdot p\right]}{1 + 0{,}0036610 \cdot t}$$

$$\delta l_{li} = L \cdot (1 - \cos\varepsilon) = L \cdot \left\{1 - \cos\left[\arctan\left(\frac{z}{L_{post}}\right)\right]\right\} = L \cdot \left\{1 - \cos\left[\arctan\left(\frac{z}{1500}\right)\right]\right\}$$

$$\delta l_{Az} = b \cdot \tan\beta = b \cdot 0{,}00003$$

$$\delta l_{Ay} = c \cdot \tan\chi = c \cdot 0{,}0000075$$

$$\delta l_{sh} = L \cdot (1 - \cos\gamma) = L \cdot \left\{1 - \cos\left[\arctan\left(\frac{h}{L_{MS}}\right)\right]\right\}$$

$$\delta l_{sv} = L \cdot (1 - \cos\varphi) = L \cdot \left\{1 - \cos\left[\arctan\left(\frac{d}{0{,}577 \cdot L_{MS}}\right)\right]\right\}$$

b – distance between line scale and laser beam in Z
c – distance between line scale and laser beam in Y
z – distance between points on laser head.

The input values x_i are defined by probability density functions $g(x_i)$ as presented in Tab. 2.

Probability density function of the output value $g(L_{MS})$ has been obtained by M = 100000 simulations and these input values z = 2 mm, b = 1 mm, c = 1 mm, h = 0,005 mm, d = 0,005 mm, $u(t)$ = 0,12 °C, $u(p)$ = 13 Pa, $u(h)$ = 0,06 i α_{MS} = $0{,}5\times10^{-6}$ 1/K. The probability density function of the output value L_{MS} for line scale of 100 mm is presented in Fig. 2.

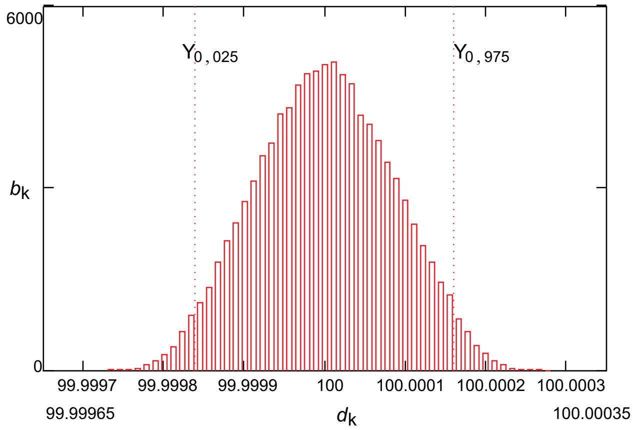

Figure 2 Probability density function $g(L_{MS})$ where s = 2 mm

The estimated standard deviations of the output value L_{MS} for line scale length of 100 mm amounts to 84 nm which confirms the uncertainty determined by the GUM method.

The output value L_{MS} is within the interval: ($Y_{0,025}$ = 99,99983996 mm; $Y_{0,975}$ = 100,000159942 mm), P = 95 %.

5 Determination of the most significant impacts of measurement uncertainty

In order to determine the most significant contribution to measurement uncertainty, probability density function of the output values L_{MS} will be simulated with different input values. For input values z = 2 mm, b = 1 mm, c = 1 mm, h = 0,005 mm, d = 0,005 mm, u(t) = 0,12 °C, $u(p)$ = 13 Pa, $u(h)$ = 0,06 and α_{MS} = $0{,}5\times10^{-6}$ 1/K simulation has been conducted and probability density function of the output value L_{MS} is shown in Fig. 2. If the distance between the points of reference and measurement laser beam on the laser head is

Table 2 Input values and probability density functions in simulating of value L_{MS}

Input value x_i		Probability density function $g(x_i)$
Refractive index of air	n_{air}	Normal distribution (M, 1, $1{,}26\cdot10^{-7}$)
Reading of interferometer 2	N_2	Rectangular distribution (M, –0,005, 0,005)
Reading of interferometer 1	N_1	Rectangular distribution (M, –0,005, 0,005)
Laser wavelength	λ	Normal distribution (M, $633\cdot10^{-6}$, $0.011\cdot633\cdot10^{-12}$)
Interferometer nonlinearity 2	δl_{n2}	Arc sine distribution (M, $-3\cdot10^{-6}$, $3\cdot10^{-6}$)
Interferometer nonlinearity 1	δl_{n1}	Arc sine distribution (M, $-3\cdot10^{-6}$, $3\cdot10^{-6}$)
Deadpath influence	δl_{DP}	Rectangular distribution (M, $-1{,}8\cdot10^{-6}$, $1{,}8\cdot10^{-6}$)
Interferometer cosine error	δl_{li}	Rectangular distribution $\left(M,\ -L\cdot\left\{1-\cos\left[\arctan\left(\frac{z}{1500}\right)\right]\right\},\ L\cdot\left\{1-\cos\left[\arctan\left(\frac{z}{1500}\right)\right]\right\}\right)$
Abbe offset in z and pitch	δl_{Az}	Rectangular distribution (M, $-b\cdot0{,}00003$, $b\cdot0{,}00003$)
Abbe offset in y and yaw	δl_{Ay}	Rectangular distribution (M, $-c\cdot0{,}0000075$, $c\cdot0{,}0000075$)
Thermal expansion coefficient	α_s	Rectangular distribution (M, $0{,}9\cdot\alpha$, $1{,}1\cdot\alpha$)
Deviation of scale temperature from 20 °C	Δt_s	Normal distribution (M, 0 °C, 0,12 °C)
Scale alignment horizontally	δl_{sh}	Rectangular distribution $\left(M,\ -L\cdot\left\{1-\cos\left[\arctan\left(\frac{h}{L_{MS}}\right)\right]\right\},\ L\cdot\left\{1-\cos\left[\arctan\left(\frac{h}{L_{MS}}\right)\right]\right\}\right)$
Scale alignment vertically	δl_{sv}	Rectangular distribution $\left(M,\ -L\cdot\left\{1-\cos\left[\arctan\left(\frac{d}{0{,}577\cdot L_{MS}}\right)\right]\right\},\ L\cdot\left\{1-\cos\left[\arctan\left(\frac{d}{0{,}577\cdot L_{MS}}\right)\right]\right\}\right)$
Scale support influence	δl_{ai}	Rectangular distribution (M, $-0{,}01\cdot L\cdot10^{-6}$, $0{,}01\cdot L\cdot10^{-6}$)
Line quality influence	δE_{alg}	Normal distribution (M, 0, $6{,}4\cdot10^{-6}$)
Focus loosing influence	δe_{fok}	Normal distribution (M, 0, $18\cdot10^{-6}$)
Uncertainty of measure. optics	δl_{opt}	Rectangular distribution (M, $-100\cdot10^{-6}$, $100\cdot10^{-6}$)
Reproducibility of line detection	δl_{sE}	Normal distribution (M, 0,11, $6\cdot10^{-6}$)

changed from z = 2 mm to z = 3 mm, then the probability density function of the output value L_{MS} appears as shown in Fig. 3.

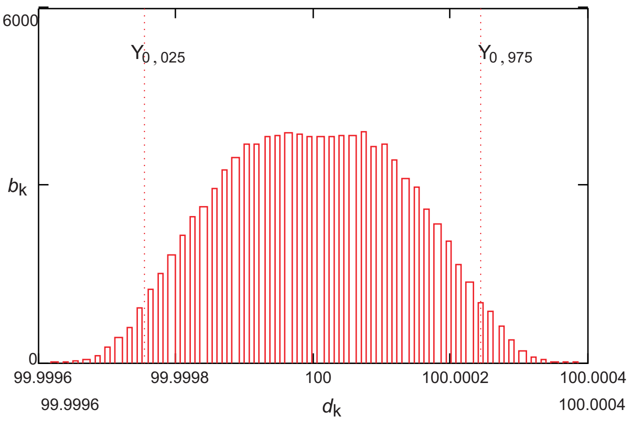

Figure 3 Probability density function $g(L_{MS})$ where z = 3 mm

The estimated standard deviation of the output value L_{MS} for line scale length of 100 mm where distance between points on laser head z = 3 mm amounts to 133 nm.

The output value L_{MS} is within the interval: ($Y_{0,025}$ = 99,99975539 mm; $Y_{0,975}$ = 100,000245649 mm), P = 95 % which is wider for 85 nm.

If the distance between points of the measuring and reference laser beam has been set at z = 5 mm, which is the maximum value because the diameter of the laser return target is equal to 5 mm then the probability density function of the output value L_{MS} looks as shown in Fig. 3. From the Fig. 3 is evident that output distribution is not normal but trapezoidal which can be attributed to the influence of the cosine error, and a rectangular distribution of the most significant input value.

The estimated standard deviation of the output value L_{MS} for line scale length of 100 mm where distance between points on laser head z = 5 mm amounts to 328 nm.

The output value L_{MS} is within the interval: ($Y_{0,025}$ = 99,99944428 mm; $Y_{0,975}$ = 100,000556157 mm), P = 95 % which is almost wider for 400 nm then interval where is z =2.

From the performed simulations is clear that cosine error significantly contributes to the measurement uncertainty so it is important to set very good alignment between laser beam and moving table.

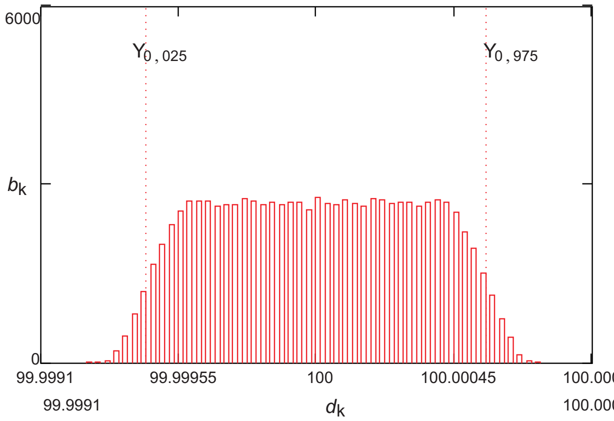

Figure 4 Probability density function $g(L_{MS})$ where z = 5 mm

If the distance between the laser beam and the line scale in both planes is increased from 1 mm to 5 mm, or if the probability density function simulates with the following parameters z = 2 mm, b = 5 mm, c = 5 mm, h = 0,005 mm, d = 0,005 mm, $u(t)$ = 0,12 ºC, $u(p)$ =13 Pa, $u(h)$ = 0,06 and α_{MS} = 0,5×10^{-6} 1/K then the probability density function of the output values L_{MS} looks as shown in Fig. 5.

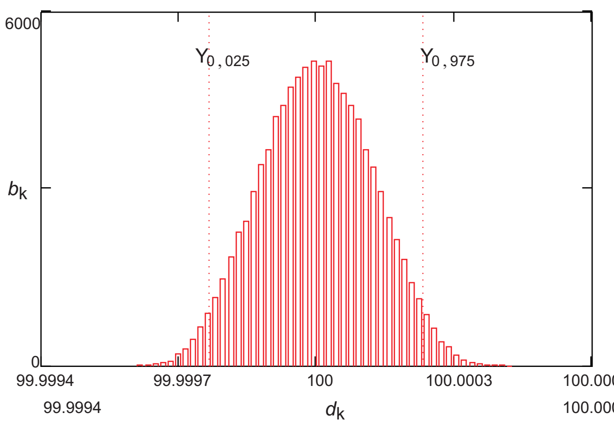

Figure 5 Probability density function $g(L_{MS})$ for line scale of 100 mm where b = 5 mm and c=5 mm

The estimated standard deviation of the output value L_{MS} for line scale length of 100 mm where z = 2 mm, b = 5 mm, c = 5 mm, h = 0,005 mm, d = 0,005 mm, $u(t)$ = 0,12 °C, $u(p)$ = 13 Pa, $u(h)$ = 0,06 and α_{MS} = 0,5×10^{-6} 1/K amounts to 120 nm. The output value L_{MS} is within the interval: ($Y_{0,025}$ = 99,99976855 mm; $Y_{0,975}$ = 100,00023162 mm), P = 95 %.

In this case the interval is wider for 70 nm, so the impact of Abbe offset in the Y and Z plane doesn't have a significant impact on measurement uncertainty as the cosine error.

If thermal expansion coefficient is changed from α_{MS} = 0,5×10^{-6} 1/K to α_{MS}=10×10^{-6} 1/K then the probability density functions of the output value L_{MS} looks as shown in Fig. 6.

The estimated standard deviations of the output value L_{MS} for line scale length of 100 mm where z = 2 mm, b = 1 mm, c = 1 mm, h = 0,005 mm, d = 0,005 mm, $u(t)$ = 0,12 °C, $u(p)$ = 13 Pa, $u(h)$ = 0,06 and α_{MS} = 10×10^{-6} 1/K amounts to 145 nm. The output value L_{MS} is within the interval: ($Y_{0,025}$ = 99,99971653 mm; $Y_{0,975}$ = 100,000284615 mm), P = 95 %.

Measurement uncertainty is increased for 120 nm and it is clear that thermal expansion coefficient has a significant impact on overall measurement uncertainty, especially at larger line scales.

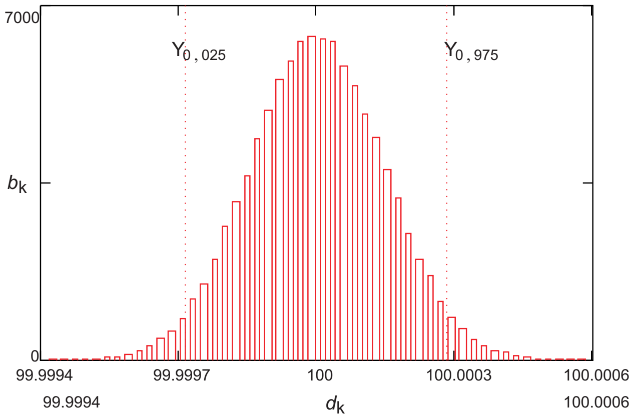

Figure 6 Probability density function $g(L_{MS})$ for line scale of 100 mm where, α_{MS}=10×10^{-6} 1/K

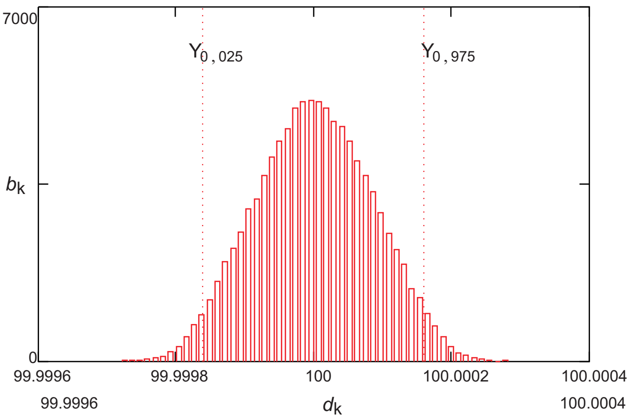

Figure 7 Probability density function $g(L_{MS})$ for line scale of 100 mm where, h=0,03 mm, d=0,03 mm

If the misalignment of line scale is increased in both planes from 0,005 mm to 0,030 mm then probability density function of the output value L_{MS} looks as shown in Fig. 7.

The estimated standard deviation of the output value L_{MS} for line scale length of 100 mm where z = 2 mm, b = 1 mm, c = 1 mm, h = 0,03 mm, d = 0,03 mm, $u(t)$ = 0,12 °C, $u(p)$ = 13 Pa, $u(h)$ = 0,06 and α_{MS} = 10×10^{-6} 1/K amounts to 84 nm. The output value L_{MS} is within the interval: ($Y_{0,025}$ = 99,999839 mm; $Y_{0,975}$ = 100,000161 mm), P = 95 %.

In this case measurement uncertainty is not changed and is equal to 160 nm, so it is clear that misalignment of line scale does not contribute significantly to the overall measurement uncertainty as a cosine error or thermal expansion coefficient of the line scale.

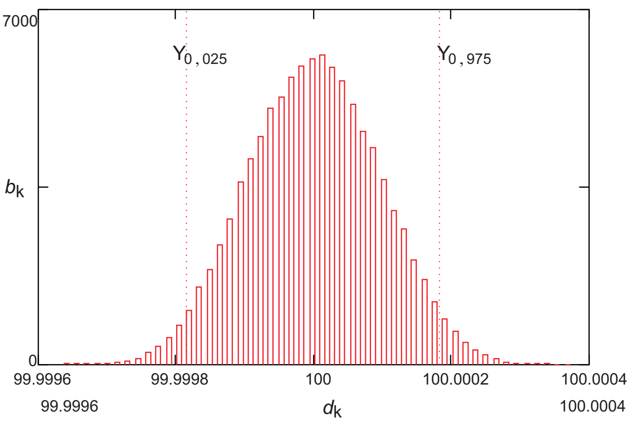

Figure 8 Probability density function $g(L_{MS})$ for line scale of 100 mm where, $u(t)$=0,5 °C

If the uncertainty of temperature measuring is increased from $u(t)$ = 0,12 °C to $u(t)$ = 0,5 °C probability density function is not significantly changed, and looks as shown in Fig. 8. In that case, the estimated standard deviation of the output value L_{MS} for line scale length of 100 mm amounts to 95 nm.

The output value L_{MS} is within the interval: ($Y_{0,025}$ = 99,999817 mm; $Y_{0,975}$ = 100,000183 mm), P = 95 %.

Measurement uncertainty is increased for only 23 nm, which implies that the uncertainty of temperature measuring has no significant impact on the measurement uncertainty of line scale calibration.

6 Validation of the device and evaluated measurement uncertainty by participation in comparison measurement

By designing the measurement system for calibration of precise line scales, the Laboratory has opened the possibility of carrying out the international comparisons in the field of line scales. Thus, the Laboratory participated in the EUROMET project 882 "Calibration of line scales", L-K7. In order to clearly determine the compatibility of Laboratory measurement results, in Tab. 3. are presented E_n values which are calculated to evaluate the compatibility of measurement results participating in the comparison measurement. Factor E_n is calculated using the following formula:

$$E_{\mathrm{n}} = \frac{x_{\mathrm{lab}} - x_{\mathrm{ref}}}{k \cdot \sqrt{u^2(x_{\mathrm{lab}}) - u^2(x_{\mathrm{ref}})}}, \tag{2}$$

where are:

k – coverage factor

x_{lab} – laboratory result

x_{ref} – referent value calculated by the formula

$$x_{\mathrm{ref}} = \frac{\sum_{i=1}^{n} u^{-2}(x_i) \cdot x_i}{\sum_{i=1}^{n} u^{-2}(x_i)}, \tag{3}$$

$u(x_{lab})$ – standard uncertainty of laboratory

$u(x_{ref})$ – referent standard uncertainty calculated by the formula

$$u(x_{\mathrm{ref}}) = \frac{1}{\sqrt{\sum_{i=1}^{n} u^{-2}(x_i)}}. \tag{4}$$

E_n value should be less than 1 that the result could be considered compatible, or if the value of E_n is closer to zero, the compatibility of that result is better.

Tab. 3. presents the calculated values x_{ref}, $u_c(x_{ref})$, deviation of measurement results from referent values and E_n values for Laboratory [8].

According to the values are shown in Tab. 3, it is evident that is achieved high compatibility of measurement results which were conducted on the system for calibration of precise line scales. From E_n values of all measured lines presented in Tab. 3., it is evident that the E_n values are far less than 1, and in most cases are near to the zero. The highest calculated value of the E_n is 0,76 for the line length of 35 mm, while the other E_n values are much lower.

Table 3 Calculated E_n values

Line /mm	x_{ref} /nm	$u_c(x_{ref})$ /nm	x_i-x_{ref} /nm	$\lvert E_n \rvert$
0,1	24,3	5,3	–21,29	0,14
0,2	1,8	5,2	–2,76	0,02
0,3	–1,2	4,9	4,16	0,03
0,4	9,8	5,7	4,21	0,03
0,5	6,6	5,2	19,38	0,13
0,6	1,7	5,0	6,28	0,04
0,7	0,5	5,2	27,51	0,18
0,8	22,7	4,9	10,29	0,07
0,9	–4,4	4,9	65,43	0,43
1	23,3	4,9	47,66	0,32
5	2,0	5,0	34,00	0,22
10	2,5	5,0	22,52	0,14
15	–7,0	5,2	–0,03	0,00
20	–2,7	5,2	16,71	0,10
25	–147,5	5,3	–90,60	0,52
30	–167,7	5,3	–108,26	0,60
35	–159,2	5,4	–139,75	0,76
40	–159,0	5,4	–8,02	0,04
45	–214,2	5,5	14,19	0,07
50	–193,4	5,5	25,42	0,13
55	–211,5	5,6	–11,78	0,06
60	–258,0	5,7	–9,67	0,05
65	–214,8	5,8	12,72	0,06
70	–245,4	5,9	–10,86	0,05
75	–282,3	5,9	–29,20	0,13
80	–240,8	6,0	–21,87	0,10
85	–269,4	8,0	–42,70	0,18
90	–429,1	6,9	38,07	0,16
95	–362,0	7,0	40,97	0,17
100	–391,0	6,3	78,99	0,32

7 Conclusion

In the presented example the Monte Carlo simulations have been primarily used for the validation of the values obtained by means of the GUM method. Example has fully confirmed the GUM values of influencing the measurement uncertainty.

While the GUM method of uncertainty calculation is based on the combining of measurement uncertainty with constant approximation to normal distribution and central limit theorem, and on that way the potential problem of determining the coverage factor k can be present, the MCS method for calculation of measurement uncertainty is based on the experimental probability density function obtained by combining different probability density functions of the input values.

The presented example confirms the advantages of the MCS method in relation to the calculation of the measurement uncertainty when the GUM method is applied. Therefore, the following may be stated for the MCS method:

1. A combination of different probability density functions is possible, which define the input values,
2. The obtained experimental PDF provide an estimate of the output value y, estimated standard deviation, and

the interval estimate
$\left(y_{\left(\left(\frac{1-P}{2}\right),M\right)}, y_{\left(\left(\frac{1+P}{2}\right),M\right)} \right)$ for the given probability P.

3. The calculation includes higher orders of the function development into Tayler's order.
4. Unknown systemic errors are simulated.

The graphical presentation of the output probability density functions has expanded the knowledge about the mentioned influences.

And finally, the participation in EURAMET Key Comparison, EURAMET.L-K7 "Calibration of line scales" was representing a real validation of the device and evaluated measurement uncertainty by GUM and MCS method.

8 References

[1] Anderson, H. L. Metropolis, Monte Carlo and the MANIAC. // Los Alamos Science, 14(1986), 96–108. http://library.lanl.gov/cgi-bin/getfile?00326886.pdf. (accessed 20.2.2012.)

[2] JCGM 101:2008 Evaluation of measurement data – Supplement 1 to the "Guide to the expression of uncertainty in measurement" – Propagation of distributions using a Monte Carlo method.

[3] Cox, M. G.; Harris, P. M. Measurement Uncertainty and the Propagation of Distributions, 10th International Metrology Congress, Saint-Louis, France, 22-25 October 2001.

[4] Raczynski, S. Uncertainty, Dualism and Inverse Reachable Sets. // Int. Journal of Simulation Modelling, 10, 1(2011), pp. 38-45.

[5] Bosse, H.; Flugge, J.; Koning, R. A method for the in situ determination of Abbe errors and their correction, Measurement science and tehnology, 18, 2007, 476-481.

[6] Santhakumar, M.; Asokan, T. Investigations on the Dynamic Station Keeping of an Underactuated Autonomous Underwater Robot. // Int. Journal of Simulation Modelling, 10, 3(2011), pp. 145-157.

[7] Mudronja, V.; Runje, B. Verification of Measurement Uncertainty by Participating in Intercomparison Measurements. // Proceedings of the 8th International scientific conference on production engineering CIM'2002, Brijuni, 2002. pp. VI-041/VI-046.

[8] Medić, S. Development of system for calibrating of line scales. // PhD work, University of Zagreb, 2011.

[9] Runje, B. The study of measurement uncertainty in the calibration procedures of length standards. // PhD work, University of Zagreb, 2002.

Authors' addresses

Dr. sc. Srđan Medić, dipl. ing.
Karlovac University of Applied Sciences
Trg J. J. Strossmayera 9
47000 Karlovac, Croatia
e-mail: smedic@vuka.hr

Doc. dr. sc. Živko Kondić, dipl. ing.
Varaždin University of Applied Sciences
J. Križanića 36
42000 Varaždin, Croatia
e-mail: zivko.kondic@velv.hr

Prof. dr. sc. Biserka Runje, dipl. ing.
Faculty of Mechanical engineering and Naval Architecture
Ivana Lučića 5
10000 Zagreb, Croatia
e-mail: biserka.runje@fsb.hr